Version of Record: https://www.sciencedirect.com/science/article/pii/S2211122015300153
Manuscript_d6c3200b441fc68d395bf62a30b8a96d

Edge-based Cuing for Detection of Benthic Camouflage

Lakshman Prasad*, Hanumant Singh**, Scott Gallager**

*Los Alamos National Laboratory, Los Alamos, NM
**Woods Hole Oceanographic Institution, Woods Hole, MA

Abstract

Locating marine organisms in their natural habitats is important for understanding ocean biodiversity. Many species are often camouflaged in their surroundings, rendering them hard to detect. Our increasing ability to image large areas of the ocean floor produces millions of images, which must be inspected to spot the occasional organism. This calls for automation of camouflage detection. We investigate reliable detectability of marine camouflage by looking for structural regularities as cues to locating organisms in their natural settings. We study skates and flounder, which use different mechanisms to avoid detection. We introduce a simple edge-based criterion for detecting local structural regularity to reduce the image area to be inspected for likely presence of camouflaged organisms. This sets the stage for efficient use of more complex algorithms to confirm detections and aid in marine census. We also study the possibility of detecting octopuses based on a simple measure of texture applied to a hierarchical segmentation of octopus images.

1. Introduction

There is a large impetus [1-3] to conduct fisheries-independent stock assessment in untrawlable areas. Such surveys might eventually negate the role of trawl surveys for bottom fish and help move the community to a non extractive method for surveying and assessing the health of various fish stock within the marine ecosystem.

In the last decade, There has been dramatic progress in the ability to collect large quantities of images from fixed and mobile (AUV, towed vehicle) camera assets. Currently our primary limitation lies in the ability to process the hundreds of thousands to millions of images that have been and are being currently collected [4-7].

While there are a number of issues that need to be addressed to make such a vision possible, one major stumbling block is that there are multiple species that are commercially important that tend to camouflage their presence on the seafloor. Species may exhibit camouflage for a variety of reasons associated with predator prey interactions, reproductive functions, etc. Related to the camouflage problem also are the issues under which the data is presented. The null case dominates—of several thousand images that are presented, only a hundred may contain camouflaged species. Of those hundred images that do contain animals, we also may have a few that may have multiple instances in the same image.

The biological mechanisms associated with camouflage are also quite varied and, as illustrated in figure 1, can easily fool attempts at detection by even highly trained users. Species exhibit spectral blending, disruption and texturing to avoid detection.

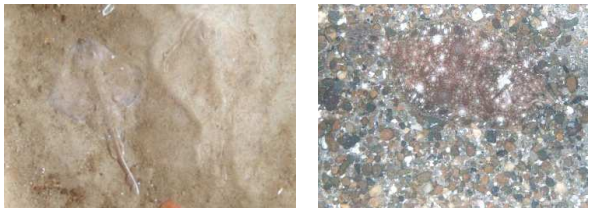

a. Two skates **b.** Flounder

Figure 1. Blending into background (**a**) and disruption (**b**)

In this paper we look for structural and spatial cues in images to detect the presence of camouflaged objects. Indeed, many animals have a certain economy of form for efficient movement, heat conservation, etc., that they cannot change easily. This structural economy manifests as local regularity of surfaces and boundaries. We therefore believe that searching for regularities in outlines and textures of features in images will provide initial clues to the possible presence of camouflaged creatures. In this paper we introduce the notion of contour compressibility that helps in effectively isolating contour fragments that are likely candidates for camouflaged animal boundaries from among thousands of contours in an image. We also describe a novel approach to texture-based discrimination in the context of detecting octopus in underwater images.

2. Background

Although image analysis is a heavily worked area, the literature on camouflage detection is relatively scant. Tankus and Yeshurun [8] leverage Thayer's principle of countershading. Thayer's principle states that some organisms use deceptive coloration to flatten their albedo,

or reflectance function, which would otherwise be convex due to body surface geometry. For example, many animals are hued darkest on their dorsal part and have gradually lighter coloration towards the sides to counteract a convex geometry that would otherwise appear brightest at the top and darker towards the limbs. Tankus and Yeshurun observe that the fact this compensation is observed in nature suggests that predators use convexity of albedo to detect prey. Accordingly, they design a filter that detects convex albedo bodies to break camouflage when this compensation is not strong or is absent. However, this method does not address camouflage that accounts for albedo flattening and other methods where blending into clutter is effected by bold, disruptive patterns of coloration to confound structural cues (Fig. 1b). Indeed, Stevens et al. [9] show that disruptive contrast is successfully used even when the patterns do not match background to confuse predators. Mayer et al. [10] study the fusion of spectral and polarimetric imagery of scenes to detect low signature targets using anomaly detection, and point out that the combination of the two modalities performs better than either one alone.

Marine imagery is largely restricted to the visible spectrum with high attenuation and scattering in other bands, making multispectral sensing and analysis impractical. Often, even in the visible range, careful color correction is needed to recover true colors. This has motivated us to investigate structural and spatial methods for deciphering camouflage. In particular, we investigate the efficacy of using image edges to detect and localize possible camouflaged organisms so that higher order algorithms may be brought to bear on select edge neighborhoods for efficient defeat of camouflage.

3. Compressibility-based edge filtering

Our premise for using edge regularity to detect camouflaged organisms is based on the observation that most organisms have a certain economy of form in their physical structure; possibly due to motile and thermal efficiency for survival. This suggests that there are likely smooth parts of their contours that could give their presence away. However, most of these organisms also have body parts such as fins, tails, or limbs that can create sharp convexities or concavities in their contours. Thus, we have to allow for such deviations from smoothness in our quest. Further, since there can be a very large number of edges detected in a benthic image due to texture and clutter, our measure of edge regularity would have to be computationally efficient to be viable for automated processing. With these considerations in mind, we formulate a simple metric of edge regularity, which we call edge compressibility. We define compressibility k of a digitized curve C as

$$k(C) = 1 - p/|C| \quad (1)$$

where p is the smallest number of points required to closely approximate a digitized curve by a polygonal line to a desired accuracy, and $|C|$ is the total number of points on the curve C. The desired accuracy is specified as the ratio of maximum deviation of the curve between two consecutive approximating points to the straight-line distance between the approximating points. In our case, we set this accuracy to 0.1. An edge detector, such as the Canny edge detector [11] is applied to an image and edges are morphologically thinned, using the default thinning algorithm in Matlab, to be a single pixel wide and chained together based on pixel adjacency to obtain contour chains based on Kovesi's Edgelink method (http://www.peterkovesi.com/matlabfns/index.html#edgelink). Each of these contour chains is a digitized curve C that will be evaluated for its compressibility $k(C)$ as defined above. The p vertices of the polygonal line approximating the curve C are chosen by 1) for each point x on C, considering a neighborhood chain of $2n$ points on C, where $n = \min(\text{ceil}(|C|/4),8)$, with n on each side of x. and 2) evaluating if that point is maximally deviant from the line segment joining the first and the last points of the neighborhood *and* if the deviation is above a specified threshold fraction (0.1) of the length of the line segment. This procedure is linear in the number of vertices comprising C. This ensures that the corners on the curve C are represented while minimally including vertices in the smooth parts. The method adapts to the saliency of the curve by allowing larger neighborhoods for longer curves to select fewer points. Other methods of polygonal approximation of digital curves may also be used to obtain similar fidelity of approximation.

An image is subjected to edge detection and the compressibility $k(C)$ of each edge pixel chain C is computed. The edges are then retained if their compressibility is above a certain percentile. Of these retained edges, only edges whose lengths are above a certain percentile (in our case, 80) are retained, resulting in a filtered set of piecewise smooth *salient* edges. This process is carried out at multiple scales of the edge detection parameter (in the case of the Canny edge detector employed in this paper, the scale is determined by the standard deviation of the Gaussian convolution kernel) to include sharp and broad edges, and the resulting retained edge sets merged to obtain a final, filtered, single-pixel wide edge set by morphological thinning. By varying the cut-off percentile of compressibility from 90 to 99, we get different edge filterings to capture the ROC performance of the filter. The choice of the length and compressibility percentile cutoffs was based on experimental and empirical observation on test data of ranges that provided a significant reduction of obtained edges while at the same time retaining some positives on camouflaged targets.

4. Performance evaluation

To evaluate our detection algorithm, we selected three sets of ground-truthed images of varying difficulty containing two kinds of camouflaged marine organisms, namely one set of 97 images containing camouflaged skates on a sandy substrate and two sets, of 71 images each, containing camouflaged flounder; one set containing sandy substrates and one set containing gravelly, cluttered substrates. The skates shallowly bury themselves in sandy substrates, while flounder display disruptive dorsal patterns that mimic clutter in their surroundings, or a subtly textured pattern in sandy surroundings. Images not containing camouflage were not used for this study. For each image (Fig 2a), ground truth was provided as a binary image with a mask represented by pixels with value one in a region that included the camouflaged organism, and zero elsewhere (Fig. 2b). Edge chains above a fixed percentile length (Fig. 2c) that fell in the mask region were deemed positives (Fig. 2d) and edges that fell outside were taken as negatives. For each threshold value of compressibility, the positives retained in an image from its 80 percentile length-thresholded edge image were taken as the true positives for that threshold value, the positives not retained were deemed false negatives, the negatives retained were considered false positives, and the negatives not retained were regarded as true negatives.

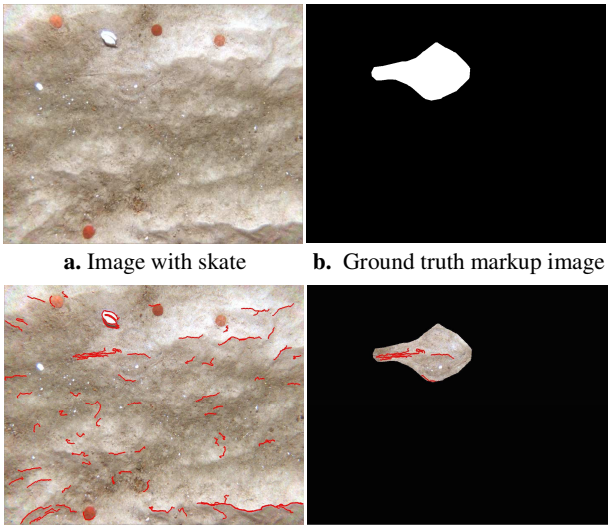

a. Image with skate **b.** Ground truth markup image

c. Edge lengths >80 percentile **d.** Deemed positive edges

Figure 2. Skate image with ground truth mask and selection of contained edges above a percentile compressibility as positives

Figure 3 shows two example images, one containing a camouflaged flounder and another, a skate. The images with red line markings are detections of contours of high compressibility, showing organism edges, along with some false alarms. Figure 4 shows the receiver operating characteristic (ROC) curves for the three data sets, where the abscissa corresponds to the False Alarm Rate = False Positives/(False Positives + True Negatives), and the ordinate corresponds to the Detection Rate = True Positives/(True Positives + False Negatives). The detector parameter (cut-off percentile of compressibility) varied to generate the ROC curves in each case was the percentile compressibility (90-99 percentile) of detected edges above a fixed percentile length (80 percentile). These results are encouraging given the difficulty of the images in the datasets, and the consistent shape of the ROC curves across the three data sets point to a common regime of optimal performance (95-97 percentile) for the two different kinds of camouflage and backgrounds.

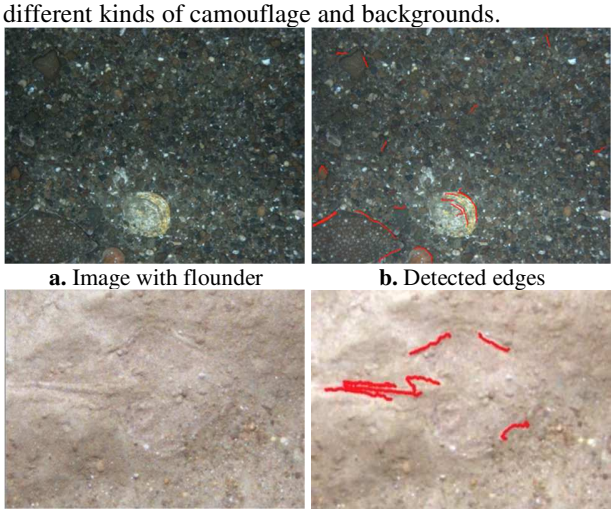

a. Image with flounder **b.** Detected edges

c. Image with skate **d.** Detected edges

Figure 3. Example detection of compressible edges of camouflaged flounder and skate

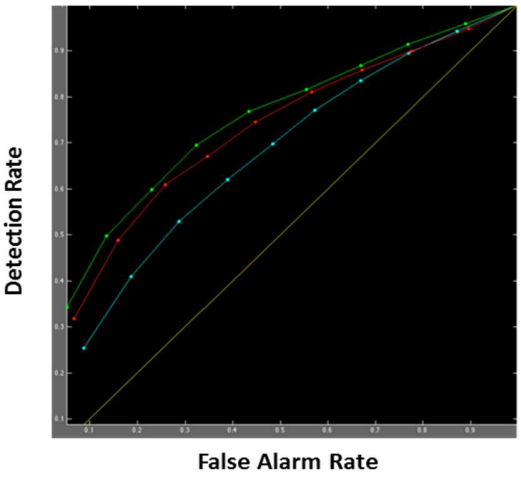

Figure 4. ROC curves for flounder and skate edge detection on the three sets (skates on sand: cyan, flounder on sand: red, and flounder on gravel: green)

Figure 5. Example detections of compressible edges of flounder in camouflage against mixed, cluttered backgrounds. The left column shows the images and the right column shows the detections in red lines. The detections illustrated here are at a threshold of 98-percentile edge compressibility, resulting in very few false positives.

Figure 6. Example detections of compressible edges of skates in camouflage against sandy backgrounds with ridges. The left column shows the images and the right column shows the detections in red lines. The detections illustrated here are at a threshold of 98-percentile edge compressibility. The presence of linear sand ridges provides ideal camouflage for the skates, which have ridges on their tails, making their detection harder.

Indeed, as we tune down the false alarm rate by increasing the compressibility percentile, we note that the targets still retain the most compressible curves even at 98-percentile compressibility (Figs. 5 & 6). This suggests that camouflage is likely consistently detectable with our notion of edge compressibility.

5. Texture-based discrimination

In contrast to the low-level detector of edge regularity that can be employed at the finest scales, we also developed a simple and efficient, higher-level, texture detector as a means of discriminating camouflaged organisms from background. Indeed, certain organisms, such as the octopus are capable of not only changing their coloration, but also their shape and surface texture to camouflage themselves amidst their surroundings. Texture is a regional property requiring evaluation of regions of images to detect changes among them. To this end, we turn to image segmentation as a means of obtaining image regions that more or less conform to image features. This ensures a degree of cohesiveness to textures by avoiding, to the extent possible, straddling of texture boundaries. Our goal is to discriminate among textures rather than robustly characterize textures individually, which is a harder problem. Textures can be thought of as being made up of agglomerations of fine-scale regions. Changes in textures can then be interpreted as changes in spatial frequency of encountering edges of these fine-scale regions as one traverses an image. To suit this model of texture discrimination, we choose a hierarchical image segmentation scheme proposed by Prasad et al [12, 13] that decomposes images into polygonal segments in a hierarchical manner, represented by a pyramidal graph. Our choice of this segmentation scheme was driven by our need for 1) subdividing features into textural elements, 2) efficiently obtaining features and their attributes from large images, and 3) a method that does not require input parameters tuning for different images. Briefly, their method groups image edges into closed contours based on proximity and smooth continuation to obtain a boundary-conforming polygonal over-segmentation at a fine scale [5]. The resulting polygons are assembled into larger polygons at subsequent levels based on perceptually driven criteria based on polygon boundary and spectral properties [13]. Polygons at each level of the hierarchy are attributed nodes in a multi-tiered graph, with boundary, color, neighborhood, parent and child attributes that make for efficient traversal and retrieval of image feature space. In this hierarchical segmentation scheme (figure 7(a)), we define the 'texturedness' of a polygon P at any given level of the hierarchy as

$$T(P) = \sum_i L(p_i)/L(P), \qquad (2)$$

where $L(p_i)$ is the perimeter of the ith polygon constituting P at the finest scale of the hierarchical segmentation, and $L(P)$ is the perimeter of the polygon P. This simple measure is inspired by Steinhaus' theorem [14] in stochastic geometry, which states that the expected number of intersections <X> of any straight line intersecting a compact planar curve Ω is given by

$$\langle X \rangle = 2L(\Omega)/CH(\Omega) \qquad (3)$$

where L(Ω) is the length of the curve Ω, and CH(Ω) is the perimeter of its convex hull (figure 7(b)). In our adaptation, we replace the perimeter of a curve Ω by the sum of perimeters of all children polygons p_i of P that are properly contained in P at the finest level of segmentation plus the perimeter of the polygon P. This is equivalent to twice the sum of all boundary arcs of the children polygons p_i *in* P. The convex hull of Ω is replaced by the perimeter of the containing parent polygon P to account for its possible non-convexity and prevent artificially increasing the number of intersections. We then subtract 1 from this modified ratio to obtain $T(P) = 0$ for a polygon with no proper children polygons., resulting in the formula (2). We take this as a measure of how "busy" the interior of a polygon is, and hence, how textured it is. The hierarchical segmentation scheme we employ readily provides us with the perimeter of each polygonal segment and its children at finer levels. So the computation of $T(P)$ is straightforward and efficient. We present this computational characterization of texture in a hierarchy more rigorously in an appendix in section 9.

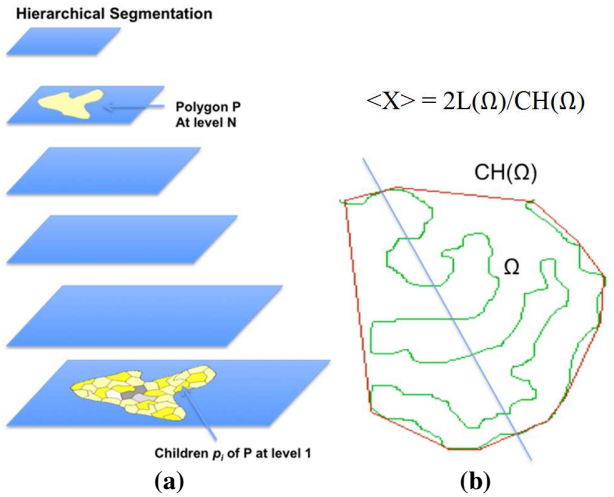

Figure 7. **(a)** Schematic of polygonal hierarchical image segmentation showing polygon P at a level N constituted of polygons p_i at level 1. **(b)** Illustration of Steinhaus theorem for planar curves.

6. Texture-based region filtering

We have applied the above measure of texturedness of

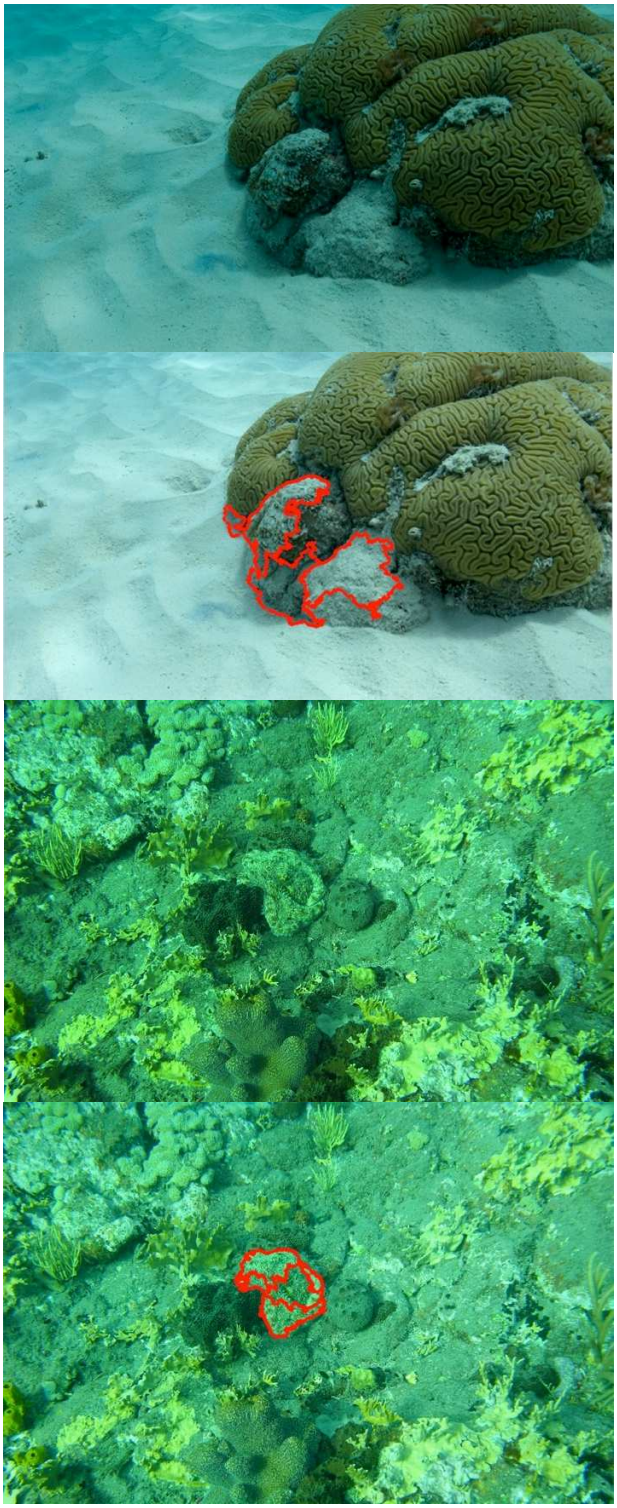

Figure 8. Images with octopus and detections using texture measure T in equation (2)

polygonal features, set out in equation (2), to images

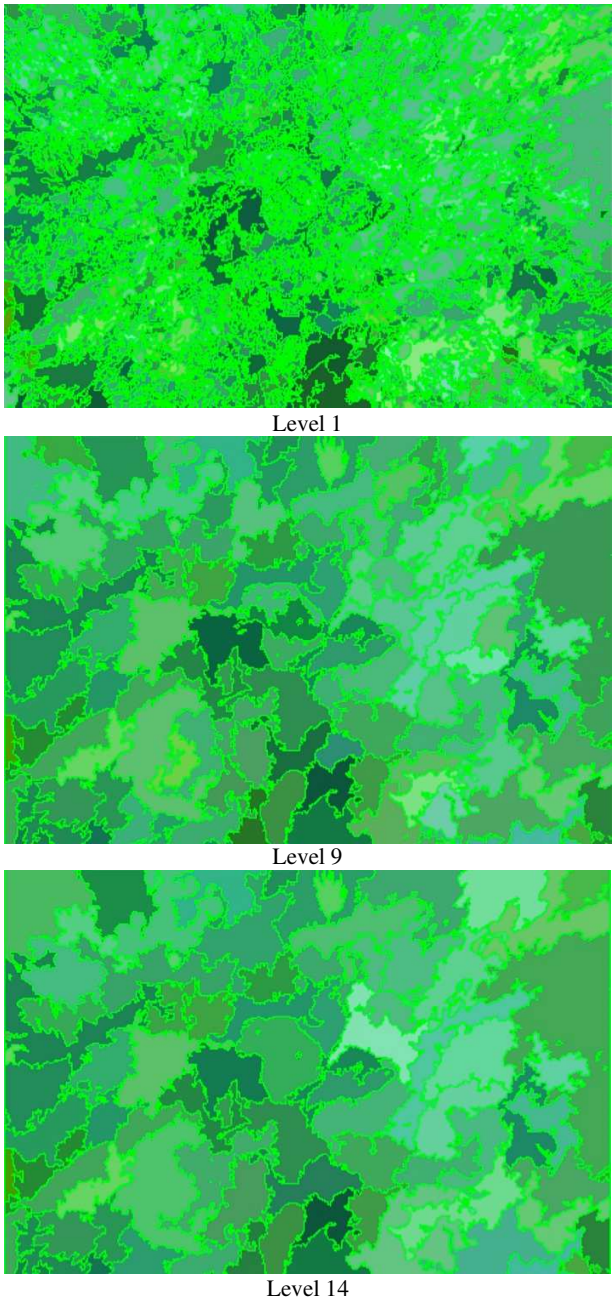

Figure 9. Three levels in the hierarchical polygonal segmentation of the second octopus image in figure 6.

containing octopus in camouflage with promising results. Since the set of such images available to us is small, we have not performed a more extensive evaluation of this approach. However, we present these early results as an example of a simple but surprisingly effective measure of textural anomalies.

Figure 8. Illustrates the application of this measure to detect octopus texturally mimicking its surroundings by wrinkling its surface. However, its wrinkles are very

uniform and create a highly textured pattern that is picked up as a maximally scoring texture.

The first octopus image in figure 8 has one correct detection and three false positives close by. This is likely because the octopus is trying to match its neighborhood texture. Thus, while we expect false positives, the filtering helps narrow down the regions of images, which are likely locations of camouflaged octopus.

7. Discussion

We have assembled over 250 images containing camouflaged organisms (skates, flounder, and octopus) that exhibit very different mechanisms of camouflage for this paper. These were carefully hand selected and ground-truth annotated for this study. We did not include null cases in this study as we were investigating the possibility of detection *given* the presence of camouflaged objects. This is because we are trying to answer the question "If there are camouflaged objects in an image, where would they most likely be?" Our methods, by the nature of their functioning, would find the most compressible edges and the most textured regions even in images not containing camouflage. However, these would all be false positives, as there are no true positives in such images. Thus, while our methods are not an oracle for detecting camouflage, they are valuable cuing mechanisms to human operators and computer algorithms to take a closer look or devote more resources, while at the same time supporting a healthy throughput of data to be processed. The benefit of cuing is to reduce the area of search, thereby increasing throughput efficiency in benthic surveys. In this study, the parameter value for selection of salient edges (80 percentile) and the compressibility percentile thresholds (90-99 percentile) were based on empirical evaluation of optimal ranges that optimally balance edge reduction and on-target edge retention.

8. Conclusion and future work

Camouflage is Nature's best approximation to invisibility. Camouflage detection is a hard and ill-posed problem. However, its importance goes beyond marine stock and health assessment. It has importance to tactical military and intelligence applications as well. A scientifically compelling reason is to obtain insights into the workings of visual perception by studying how it is confounded and when/why it breaks down. In spite of significant advances in image analysis and computer vision, camouflage detection is beyond our current reach. In this paper, we have attempted to address the challenge by examining if camouflage, in its various manifestations, has a vulnerability that we can exploit to defeat it. The approach and filters we have introduced here are meant to be cuing mechanisms that help tractable and efficient search for camouflage in vast amounts of data-the proverbial needle in a haystack problem. Therefore, it is imperative that the cuing methods be cheap and fast to allow for efficient deployment of more computationally complex and sophisticated algorithms to focus attention on high probability areas. Camouflage confounds our perceptual expectations by spectral blending or disruption. There is some evidence that certain colorblind people may fare better at deciphering camouflage [15]. Our approach avoids spectral information and targets spatial and structural aspects of features instead, to address camouflage detection.

It is our hope that this fledgling but promising work in camouflage detection will inform and inspire other researchers in the computer vision community to address this challenging problem. The available camouflage data is currently sparse, but with advances in underwater robotic and towed vision platforms there will be significant opportunities to address camouflage detection in all its aspects and applications.

Our future work will focus on combining edge and texture-based cuing along with other spatial regularity filters such as local symmetry detection (e.g., Patraucean et al [16]), which may be more computationally intensive, to look for nonaccidental statistics [17] in images that reinforce detectability. Spectral processing in cued regions, at least for underwater imagery, still requires color correction. However, with improved color correction algorithms, spectral processing to confirm detections adds another dimension to camouflage defeat. Another important cuing mechanism that is fast becoming viable is stereoscopic depth perception via stereo cameras that will provide relief information. We will investigate the efficacy of depth from disparity in detecting camouflage.

9. Appendix: Measuring texture via a hierarchical image segmentation

Given a raster image *I*, the hierarchical polygonal segmentation employed in this paper yields a pyramidal graph H_I that consists of $N \geq 1$ levels of segmentation into polygons. We denote the *j*th polygon at the *i*th level by $H_I(i, j)$, and the inclusion of its interior by $\overline{H_I(i, j)}$. The level-*k* *descendants* of $H_I(i, j),\ i > 1,$ at a finer level $k < i$ are polygons $H_I(k, m)$ such that

$$\overline{H_I(i, j)} = \bigcup_{m=i_1}^{i_j} \overline{H_I(k, m)} \tag{4}$$

Steinhaus' theorem on the expected number $\langle X \rangle$ of intersections of a straight line intersecting a compact planar curve Ω states that

$$\langle X \rangle = \frac{2L(\Omega)}{CH(\Omega)}$$

(5)

Where $L(\Omega)$ is the length of the curve Ω, and $CH(\Omega)$ is the perimeter of the convex hull of Ω.
In our paper, we model our measure of texture based on the above elegant and simple to compute formula. We adapt it to the case of nested polygons in the hierarchical segmentation as follows:

1) We replace the numerator of the RHS of equation (5) by the sum of the perimeters of all *proper* level-1 descendants $H_I(1,m) \subset H_I(i,j), m \in \{k_1,...,k_j\}$ of a level-*I* olygon $H_I(i,j)$ plus the perimeter $P(H_I(i,j))$ of the polygon $H_I(i,j)$. This has the effect of taking into consideration twice the lengths of boundary segments of all level1descendant polygons of $H_I(i,j)$.
2) We replace the denominator of the RHS of equation (2) by the perimeter $P(H_I(i,j))$ of the polygon $H_I(i,j)$ whose texturedness we are interested in measuring.

3) Finally, we subtract 1 from this ratio to obtain a texture value of zero when the level-1 descendant of $H_I(i,j)$ is itself. That is, when $H_I(1,m) = H_I(i,j)$ for some single value of *m*.

Indeed, division by the perimeter $P(H_I(i,j))$, which is also the outer perimeter of the level-1 descendants of the polygon of interest rather than by its convex hull is to avoid a nonzero texture measure when $H_I(1,m) = H_I(i,j)$. This helps adapt the measure to non-convex polygons without artificially boosting their texturedness due to their nonconvexity. Thus, our measure of texturedness of the *j*th polygon $H_I(i,j)$at level *i* of the hierarchical polygonal segmentation H_I of an image *I* is given by

$$T(H_I(i,j)) = \frac{\sum_{H_I(1,m) \subset H_I(i,j)} P(H_I(1,m))}{P(H_I(i,j))}$$

(6)

In our empirical study of the effectiveness of this measure in capturing octopuses as highly textured objects, we applied it at a level *I* in the hierarchy at which the median number of level-1 descendants per polygon exceeded the total number of polygons at level *I* for the first time. This was to avoid evaluating polygons prematurely for texture before the polygon agglomeration process precipitated textured segments in the hierarchy.
Upon choosing such a level *I*, we selected polygons at or above the 98th percentile as candidate octopus detections in our study.
We observe that apart from wrinkling its skin to texturally blend into its immediate surroundings, the octopus also has relatively compact, if not convex, form. This reduces the perimeter of the polygon delineating (e.g., at level 14 of figure 9 in the paper) the octopus, thereby giving it a higher texture value than otherwise. This may also be a factor in helping distinguish it from surrounding vegetative textures, which are more ramified in shape.
This work was supported in part by research grants from the Gordon & Betty Moore Foundation Grant # 2649, subaward No. A101036, and NOAA fisheries under their Automated Image Analysis Strategic Initiative .

References

[1] Allen, L. G., Pondella, D. J., and Shane, M. A., "Fisheries independent assessment of a returning fishery: Abundance of juvenile white seabass (Atractoscion nobilis) in the shallow nearshore waters of the Southern California Bight, 1995–2005." Fisheries Research 88.1 (2007): 24-32.
[2] Yoklavich, M. M., Love, M. S. and Forney, K. A., "A fishery-independent assessment of an overfished rockfish stock, cowcod (Sebastes levis), using direct observations from an occupied submersible." Canadian Journal of Fisheries and Aquatic Sciences 64.12 (2007): 1795-1804.
[3] NOAA Untrawlable Habitat Strategic Initiative http://www.afsc.noaa.gov/Quarterly/JFM2015/jfm15feature.htm accessed April 28, 2016.
[4] Clarke, E. M., Tolimieri, N., and Singh, H., "Using the seabed AUV to assess populations of groundfish in untrawlable areas." The future of fisheries science in North America. Springer Netherlands, 2009. 357-372.
[5] Tolimieri, N, et al. "Evaluating the SeaBED AUV for monitoring groundfish in untrawlable habitat." Marine habitat mapping technology for Alaska (2008): 129-141.
[6] Williams, Stefan B., et al. "AUV benthic habitat mapping in south eastern Tasmania." Field and Service Robotics. Springer Berlin Heidelberg, 2010.
[7] Howland, Jonathan, et al. Development of a towed survey system for deployment by the fishing industry. Proceedings of the IEEE Oceans Conference, 2006.
[8] Tankus, A., and Yeshurun, Y., "Computer vision, camouflage breaking and countershading", Phil. Trans. R. Soc. B vol. 364 no. 1516 529-536 (2009).
[9] Stevens, M., Cuthill, I.C., Windsor, A. M. M., and Walker, H. J., "Disruptive contrast in animal

camouflage", Proc. Trans. R. Soc. B vol. 273 2433-2438 (2006).
[10] Mayer, R., Priest, R., Stellman, C., Hazel, G., Schaum, A., Schuler, J., and Hess, M., "Detection of camouflaged targets in cluttered backgrounds using fusion of near-simultaneous spectral and polarimetric imaging," Proc. Meeting of the MSS Specialty Group on Passive Sensors, Vol. 1, Naval Research Lab Washington Dc Optical Sciences Div (2000).
[11] Canny, J., "A computational approach to edge detection," IEEE Transactions on PAMI, vol. 8, no. 6, pp. 679–698, 1986.
[12] L. Prasad, A. N. Skourikhine, Vectorized Image Segmentation via Trixel Agglomeration, Pattern Recognition vol. 39, Issue 4, pp 501-514, April 2006.
[13] Prasad, L., and Swaminarayan, S., "Hierarchical image segmentation by polygon grouping," Proceedings of the IEEE CVPR Workshop on Perceptual Organization in Computer Vision, Anchorage, AK. (2008).
[14] Santalo, L. A., "Integral Geometry and Geometric Probability", Encyclopaedia of Mathematics and its Applications 1 (Addison Wesley, 1976) page 31.
[15] Morgan, M. J., Adam, A., and Mollon, J. D., "Dichromats detect colour-camouflaged objects that are not detected by trichromats", Proc. Biol. Sci, Jun 22; 248 (1323) 291-5, 1992.
[16] Patraucean, V., von Gioi, R.G., and Ovsjanikov, M., "Detection of Mirror-Symmetric Image Patches", Proceedings of IEEE CVPR 2013.
[17] Zhu, S-C., "Embedding Gestalt Laws in Markov Random Fields", IEEE Trans. PAMI, Vol. 21 (11), 1170-1187, 1999.